HHS Public Access

Author manuscript

Int J Cardiol. Author manuscript; available in PMC 2017 December 15.

Published in final edited form as:

Int J Cardiol. 2016 December 15; 225: 371–380. doi:10.1016/j.ijcard.2016.10.021.

Junctophilin-2 gene therapy rescues heart failure by normalizing RyR2-mediated Ca^{2+} release

Julia O. Reynolds, BS[1,2,*], **Ann P. Quick, BA**[1,2,*], **Qiongling Wang, PhD**[1,2,*], **David L. Beavers, MD, PhD**[1,3], **Leonne E. Philippen, MSc**[1,2], **Jordan Showell, BS**[1,2], **Giselle Barreto-Torres, PhD**[1,2], **Donna J. Theurauf**[6], **Shirin Doroudgar**[7,8], **Christopher C. Glembotski, PhD**[6], and **Xander H.T. Wehrens, MD, PhD**[1,2,4,5]

[1]Cardiovascular Research Institute, Baylor College of Medicine, Houston, TX 77030, USA

[2]Dept. of Molecular Physiology & Biophysics, Baylor College of Medicine, Houston, TX 77030, USA

[3]Translational Biology and Molecular Medicine Program, Baylor College of Medicine, Houston, TX 77030, USA

[4]Dept. of Medicine/Cardiology, Baylor College of Medicine, Houston, TX 77030, USA

[5]Dept. of Pediatrics, Baylor College of Medicine, Houston, TX 77030, USA

[6]San Diego State University Heart Institute and Department of Biology, San Diego State University, San Diego, CA 92182, USA

[7]Department of Cardiology, Angiology, and Pneumology, University Hospital Heidelberg, Innere Medizin III, Im Neuenheimer Feld 669, 69120 Heidelberg, Germany

[8]DZHK (German Centre for Cardiovascular Research), Partner Site Heidelberg/Mannheim, 69120 Heidelberg, Germany

Abstract

Background—Junctophilin-2 (JPH2) is the primary structural protein for coupling of transverse (T)-tubule associated cardiac L-type Ca channels and type-2 ryanodine receptors on the sarcoplasmic reticulum within junctional membrane complexes in cardiomyocytes. Effective signaling between these channels ensures adequate Ca-induced Ca release required for normal cardiac contractility. Disruption of JMC subcellular domains, a common feature of failing hearts, has been attributed to JPH2 downregulation. Here, we tested the hypothesis that adeno-associated virus type 9 (AAV9) mediated overexpression of JPH2 could halt the development of heart failure in a mouse model of transverse aortic constriction (TAC).

Address for Correspondence: Xander H.T. Wehrens, MD, PhD, Baylor College of Medicine, One Baylor Plaza, BCM335, Houston, TX 77030, United States, Tel: 713-798-4261; Fax: 713-798-3475; wehrens@bcm.edu.

*These authors contributed equally to this work.

6. CONFLICT OF INTEREST

None declared.

Methods and Results—Following TAC, a progressive decrease in ejection fraction was paralleled by a progressive decrease of cardiac JPH2 levels. AAV9-mediated expression of JPH2 rescued cardiac contractility in mice subjected to TAC. AAV9-JPH2 also preserved T-tubule structure. Moreover, the Ca^{2+} spark frequency was reduced and the Ca^{2+} transient amplitude was increased in AAV9-JPH2 mice following TAC, consistent with JPH2-mediated normalization of SR Ca^{2+} handling.

Conclusions—This study demonstrates that AAV9-mediated JPH2 gene therapy maintained cardiac function in mice with early stage heart failure. Moreover, restoration of JPH2 levels prevented loss of T-tubules and suppressed abnormal SR Ca^{2+} leak associated with contractile failure following TAC. These findings suggest that targeting JPH2 might be an attractive therapeutic approach for treating pathological cardiac remodeling during heart failure.

Keywords

Calcium; cardiomyopathy; heart failure; junctophilin; gene therapy; T-tubule

1. INTRODUCTION

Heart failure (HF) is a progressive disease marked by the inability of cardiac output to keep up with systemic metabolic demands. Efficient excitation-contraction coupling (ECC) is critical for normal cardiac contractility [1]. Critical to normal ECC are the complex and highly ordered junctional membrane complexes (JMC), where sarcolemmal invaginations known as transverse (T)-tubules are anchored to junctional sarcoplasmic reticulum (SR). Within these 12–15 nm clefts, plasmalemmal voltage-activated L-type Ca^{2+} channels (LTCC) are coupled to SR associated type-2 ryanodine receptors (RyR2) [2].

With cardiomyocyte depolarization, a small influx of Ca^{2+} through LTCC triggers a greater efflux of Ca^{2+} from SR stores through RyR2, a physiological process known as Ca^{2+}-induced Ca^{2+} release (CICR). This increase in cytosolic Ca^{2+} levels promotes sarcomeric cross-bridge formation and myocyte contraction. Upon relaxation, Ca^{2+} is extruded from the cell via the Na^{+}/Ca^{2+} exchanger (NCX), and pumped back into SR stores by the sarco/endoplasmic reticulum Ca^{2+}-ATP-ase (SERCA2a). Junctophilin-2 (JPH2) is a key cardiac structural protein critical in forming and maintaining JMCs by acting as a spacer molecule within the dyadic space [3]. In addition to this structural role, JPH2 has been shown to directly interact with and stabilize RyR2 [4, 5].

Loss of this well-organized T-tubule network has been observed during the progression of cardiac disease towards decompensated HF of various etiologies [6, 7]. Several studies have shown that downregulation of JPH2 protein levels may be an early molecular event preceding such pathological remodeling in both animal models and humans [8, 9]. Moreover, acute loss of JPH2 in adult mice resulted in HF and increased mortality [5].

On the other hand, increased levels of JPH2 in transgenic mice with cardiac-specific JPH2 overexpression (JPH2-Tg) were shown to be protective against the effects of pathological stress in a mouse model of HF [3, 5, 10]. However, it is currently unknown whether restoring JPH2 levels in mice with experimental HF could prevent disease progression. Therefore, we

developed a novel adeno-associated virus (AAV9)-mediated gene therapy approach to re-express JPH2 in the hearts of mice with mild HF as a result of transverse aortic constriction (TAC). Our results revealed that restoration of cardiac JPH2 levels prevented the progressive development of cardiac failure after TAC observed in another group of mice receiving a negative control AAV9. Thus, normalizing JPH2 levels appears to be a promising therapeutic target for the prevention of HF development in preclinical studies.

2. METHODS

2.1. Study Animals

All animal procedures were conducted with approval of the Institutional Animal Care and Use Committee of Baylor College of Medicine, and conform to the Guide for the Care and Use of Laboratory Animals published by the U.S. National Institutes of Health (NIH Publication No. 85-23, revised 2011). Three to four-month old male C57BI/6J mice were used for shams and TAC gene therapy studies.

2.2. Mouse TAC model

Mice were anesthetized using 2% isoflurane mixed with 100% O_2 (0.8 L/min) and anesthesia was maintained at 1.5–2% isoflurane by endotracheal intubation and ventilation throughout the procedure. The aortic arch was visualized by performing an anterior thoracotomy to the level of the third intercostal space. Constriction was performed by tying a 6-0 silk suture against a 28-gauge needle between the first and second trunk of the aortic arch. For consistency, constriction levels were quantified by measuring alterations in Doppler velocities of the right and left carotid arteries 7 days post-surgery. Right-to-left carotid peak velocity ratios ranged from 5.0 to 6.5 and 2-week post TAC ejection fractions ranged from 40%–50% in TAC groups used for gene therapy.

2.3. Transthoracic Echocardiography

Mice were anesthetized using 1.5% isoflurane in 100% O_2 at 1.5 L/min. Vital signs were continuously monitored to ensure similar heart and respiration rates. Body temperature was maintained between 36.5–37.5°C on a heated platform. Cardiac function was measured using a VisualSonics VeVo 2100 Imaging System (VisualSonics, Toronto, Canada) equipped with high-frequency MS505 probe, as described [11].

2.4. Western Blotting

Tissue lysates were made from hearts flash frozen in liquid nitrogen by pulverization followed by sonication in Radio-Immunoprecipitation Assay (RIPA) lysis buffer containing 10% CHAPS, 20 mM NaF, 1 mM Na_3VO_4, and 1× protease and phosphatase inhibitor tablets (Roche Diagnostics, Indianapolis, IN) each dissolved in 1mL water. Cellular debris was cleared from lysate by centrifugation (16,000 g for 25 min at 4°C). 75 μg of total protein was diluted in 2× Laemmli sample buffer (Bio-Rad, Hercules, CA) containing 5% β-mercaptoethanol, heated to 70°C for 10 minutes and resolved on a 6–12% gradient sodium dodecyl sulfate (SDS) polyacrylamide electrophoresis gel. Proteins were electrotransferred to polyvinylidene difluoride (PVDF).

Membranes were blocked in 5% milk tris-buffered saline (TBS) for 1 hour. Primary antibody was suspended in 5% milk TBS solution and incubated with membranes for 3 hours at room temperature or overnight at 4°C followed by incubation in a 1:10,000 dilution of fluorescent secondary antibody (Alexafluor 680 anti-mouse IgG, Invitrogen or IRDye800 conjugated anti-rabbit IgG, Rockland) for 60 min at room temperature. Primary antibodies consisted of a custom polyclonal rabbit anti-JPH2 antibody (1:1,000), and monoclonal mouse anti-GAPDH (1:10,000, MAB374, Millipore). Blots were imaged using a Licor Odyssey two channel IR fluorescence scanner.

2.5. Adeno-associated virus gene delivery

An adeno-associated virus type 9 (AAV9) containing full length JPH2 expression vector (AAV9-JPH2) or MLC800 control vector (AAV9-Con) were generated in the lab of Dr. Christopher Glembotski (Department of Biology, San Diego St. University, San Diego, CA) using previously published methods [12]. Three weeks after TAC, 1×10^{11} genome containing units of AAV9 suspended in lactated ringers solution was administered via tail-vein injection in anesthetized mice.

2.6. Myocyte isolation

After euthanizing mice under Isoflurane anesthesia, hearts were removed and rinsed in 0 Ca Tyrode solution (137 mm NaCl, 5.4 mm KCl, 1 mm $MgCl_2$, 5 mm HEPES, 10 mm glucose, 3 mM NaOH, pH 7.4). The heart was cannulated through the aorta and perfused on a Langendorff system briefly with 0 Ca Tyrode, then 0 Ca Tyrode containing 20 μg/ml (0.104 a.u./ml) Liberase TH Research Grade (Roche Applied Science) was applied to digest the heart at 37 °C. After digestion, the heart was rinsed with 5 ml Kreb's buffer (KB) solution (90 mM KCI, 30 mM K_2HP0_4, 5 mM $MgSO_4$, 5 mM pyruvic acid, 5 mM β-hydroxybutyric acid, 5 mM creatine, 20 mM taurine, 10 mM glucose, 0.5 mM EGTA, 5 mM HEPES, pH 7.2) to wash out collagenase. Ventricles were minced in KB solution and gently agitated, then filtered through a 210 mm polyethylene mesh. After settling, ventricular myocytes were washed once with KB solution, and stored in KB solution at room temperature before use.

2.7. Confocal Ca^{2+} and T-tubule imaging

Ventricular myocytes were either incubated at room temperature for 20 minutes with 10 μM Di-8-ANNEPS to visualize T-tubules or 2 μM Fluo-4-acetoxymethyl ester (Fluo-4 AM, Invitrogen) in normal Tyrode solution containing 1.8 mM Ca^{2+} for 60 minutes for Ca^{2+} imaging. Cells were transferred to a chamber equipped with a pair of parallel platinum electrodes on a laser scanning confocal microscope (LSM 510, Carl Zeiss) with a 40× oil immersion objective. Fluo-4 AM was excited at 488 nm with emission collected through a 515 nm long pass filter. Fluorescence images were recorded in line-scan mode with 1024 pixels per line at 500 Hz. After being paced at 1 Hz (5 ms at 10 V) for 2 minutes, only myocytes showing clear striation and normal contractility were selected for further experiments. Once steady state calcium transient was observed, pacing was paused for 30 seconds to record Ca^{2+} sparks.

T-tubules were analyzed using Fourier transformation in ImageJ and Ca^{2+} spark parameters were analyzed using the ImageJ plugin SparkMaster program [13]. The threshold for

detection of Ca^{2+} spark events was 3.8 times the standard deviation of the background noise over the mean value of the background.

2.8. Quantitative polymerase chain reaction (qPCR)

Following flash freezing in liquid nitrogen, pulverized hearts were lysed in TRIzol-Reagent (Thermo Fisher Scientific) and mRNA was isolated using the Directzol RNA Miniprep Kit (Zymogen). cDNA was synthesized by reverse transcription of 1 μg mRNA using iScript (Biorad) and diluted 1:10. Transcripts were quantified by mixing PerfeCTASYBR Green (Quanta), 1μL diluted cDNA, and the appropriate primer sets followed by thermal cycling in an Eppendorf realplex^2 Mastercyler. The following primer sequences listed in the 5′ to 3′ direction were used: *L7* forward: GAAGCTCATCTATGAGAAGGC, L7 reverse: AAGACGAAGGAGCTGCAGAAC, *Nppa* forward: TCTTCCTCGTCTTGGCCTTT, *Nppa* reverse: CCAGGTGGTCTAGCAGGTTC, *Nppb* forward: CTCTGGGAAGTCCTAGCCAG, *Nppb* reverse: CTGCCTTGAGACCGAAGGAC, *Myh7* forward: GAGCTGGGAAGACTGTCAAC, Myh7 reverse: CGAGAGGAGTTGTCATTCCG, *Actal* forward: CTGAGCGTGGCTATTCCTTC, Actal reverse: CATTGCCGATGGTGATGACC, *Rcanl.4* forward: CATGCAGCGACAGACACCAC, *Rcan1.4* reverse: GTGGATGGGTGTGTACTCCG.

2.9. Statistical analysis

Results are expressed as mean ± standard error of the mean (±). Data were analyzed using Graphpad Prism software by one-way ANOVA with Tukey post-test to compare means of 3 groups. Paired T-tests were used to determine differences between the same group over time. Student's T-tests were used to determine differences between 2 groups at the same time point.

3. RESULTS

3.1. Pressure-overload induced HF leads to decline in JPH2 expression

Although a prior study demonstrated a reduction in JPH2 levels in an animal model of HF [14], the exact correlation between the degree of systolic dysfunction and the level of cardiac JPH2 levels was not explored. Here, we performed TAC on mice, and assessed cardiac function using echocardiography at predefined time points (Fig. 1A). Sham-operated mice, which were subjected to the same procedure without banding the aorta, were used as controls. The degree of aortic constriction was assessed at 1-week post-TAC using Doppler, and the ratio between right carotid artery to left carotid artery peak blood flow velocity (RC/LC) was measured (Fig. 1B). As expected, there was a reasonable correlation between the RC/LC ratio and the cardiac ejection fraction (EF) measured at 8-weeks post-TAC.

Mice were sacrificed at 8-weeks post-TAC and divided into three groups. Mice that developed an EF between 40–60% were considered to have early-stage HF, whereas mice with EF from 25–39%, and <25% were considered to have moderate and severe HF, respectively. Western blots revealed that JPH2 levels are significantly decreased in TAC mice with moderate and severe HF (Fig 1C–D). Based on this evidence, we hypothesized

that intervention in the early stages of HF using JPH2 gene therapy would prevent JPH2 loss and development of HF with a reduced EF.

3.2. Adeno-associated virus serotype 9 (AAV9)-mediated JPH2 gene therapy increases JPH2 protein levels in mouse hearts

To selectively overexpress JPH2 in cardiomyocytes, we developed AAV9 constructs, based on the pTRUF vector driven by a cardiac-specific MLC2v800 promoter, as previously described [15][, containing either a hemagglutinin (HA)-tagged JPH2 sequence (AAV9-JPH2) or empty vector control (AAV9-Con) flanked by inverted terminal repeats (ITR) (Fig 2A). These constructs were injected into wild-type mice through the tail vein, hearts were collected after two weeks to assess JPH2 protein levels using western blotting (Fig. 2B). Compared to AAV9-Con treated mice, JPH2-AAV9 treatment increased cardiac JPH2 protein expression levels by 2.38 ± 0.61% ($P<0.12$) (Fig 2B–C).

3.3. Design for gene therapy study in a mouse model of HF

Based on our pilot study demonstrating a correlation between loss of JPH2 expression and HFdevelopment following TAC, we designed a pre-clinical trial in which mice with moderate TAC were randomized to receive either AAV9-JPH2 or AAV9-Con therapy (Fig. 3A). All mice entering the study (N=77) received baseline echocardiography and then underwent TAC (N=67) or sham (N=10) surgery. Thirteen TAC mice died during or after surgery, leaving 54 surviving TAC mice (Fig. 3B). In order to assess the degree of aortic constriction during TAC surgery, Doppler ratios of right carotid to left carotid peak velocity (RC/LC) were determined at one-week post-TAC. Thirty-four TAC mice with RC/LCs ranging from 5.0–6.5 were included, because prior studies from our lab have demonstrated that this level of constriction commonly leads to progressive development of HF [16, 17]. The remaining 20 mice that did not meet the Doppler criteria were excluded from the study.

Subsequently, echocardiograms at 2-week post-TAC were used to further assess TAC severity. Of the remaining 34 mice, 10 were excluded with EFs outside the range of 40–50%, because they either did not develop HF or already exhibited signs of more severe HF (Fig. 3C). Twenty-four mice within a consistent Doppler and 2-week post-TAC EF range entered the prospective, randomized trial in which mice were assigned either AAV9-JPH2 (N=11) or AAV9-Con (N=13) treatment. The AAV9 was delivered by tail-vein injection at 3-weeks post TAC. Following AAV9 treatment, mice underwent serial echocardiography at 5, 7, and 9 weeks post TAC corresponding to 2, 4, and 6 weeks post AAV9 intervention (Fig 3A).

3.4. AAV9-JPH2 gene therapy maintains cardiac function after pressure-overload induced pathological remodeling

To determine whether JPH2 may be a clinically relevant therapeutic intervention for HF, we tested the effects of JPH2 overexpression *after* the onset of moderate cardiac dysfunction. Sham-operated mice were used as controls, and had similar cardiac function as assessed by echocardiography compared to TAC mice at baseline (Table 1). Moreover, the sham group maintained cardiac function throughout the study (Table 2). Therefore, we will focus on the

comparison between AAV9-Con and AAV9-JPH2 treated animals in the remainder of this section.

Mice subjected to TAC displayed a significant decline in cardiac function by 2-weeks post-TAC with an average EF of 45.4 ± 0.5% compared to baseline (69.5 ± 1.0%; P<0.0001). Following AAV9 administration, the EF of AAV9-Con treated mice continued to decline whereas, AAV9-JPH2 treated mice maintained EF levels similar to those at 2-weeks after TAC (Fig. 4B). Starting 2 weeks after AAV9 treatment (i.e., 5 weeks post-TAC), mice receiving AAV9-JPH2 had a significantly increased EF (49.0 ± 2.0%, N=11) compared to the AAV9-Con group (37.7 ± 2.5%, N=13, P=0.03) (Figure 4A–B). By 6 weeks after treatment (i.e., 9 weeks post-TAC), AAV9-JPH2-treated mice maintained an improved EF (47.2 ± 2.9%, N=11) over AAV9-Con (29.4 ± 2.1%, N=13, P<0.0001). Whereas cardiac function in mice that received AAV9-Con declined progressively with time after TAC (from 45.0 ± 0.7% at 2 weeks to 29.4 ± 2.1% at 9-weeks post-TAC; P<0.0001), mice treated with AAV9-JPH2 were protected from impairment in cardiac function (45.8 ± 0.6% at 2-weeks vs. 47.2 ± 2.9% at 9-weeks post-TAC; P=0.65; Figure 4B).

Mice that underwent TAC surgery and were treated with AAV9-Con developed left ventricular chamber dilation, as evidenced by an increased end-diastolic diameter (Figure 4C). In contrast, mice that received AAV9-JPH2 did not show signs of dilation of the left ventricle. At 9-weeks post-TAC, AAV9-JPH2 treated mice had a significantly lower mean EDD (4.23 ± 0.10 mm, N=11) compared to AAV9-Con treated mice (4.77 ± 0.17 mm, N=13, P=0.01. Figure 4C).

Finally, AAV9-JPH2 treated mice demonstrated thickened walls compared to AAV9-Con treated mice by 9-weeks post-TAC. This is exemplified by thicker systolic posterior wall thickness (LVPW;s) in AAV9-JPH2 treated mice (1.45 ± 0.03 mm, N=11) versus AAV9-Con mice (1.20 ± 0.05 mm, N=13, P=0.007, Figure 4D). These data strongly suggest that overexpression of JPH2 by AAV9 *after* the onset of pathological left ventricular remodeling can preserve cardiac function and prevent systolic HF development after pressure overload in mice.

3.5. AAV9-JPH2 therapy attenuates transverse-tubule (T-tubule) remodeling in TAC mice

In order to determine whether T-tubule architecture was preserved in parallel with cardiac function in AAV9-JPH2 treated mice, we studied ventricular myocytes isolated from sham mice, and AAV9-Con and AAV9-JPH2 treated TAC mice (Fig. 5A). First, cardiomyocyte size did not change significantly between groups (Figure 5B). However, the T-tubular structure was notably affected as a result of cardiac remodeling following TAC. The T-tubule area was significantly lower AAV9-Con treated TAC mice (0.23 ± 0.01 μm^2) compared to the T-tubule area in sham mice (0.29 ± 0.01; P<0.0001; Fig. 5C). Treatment with AAV9-JPH2, however, restored the T-tubule area to levels similar to sham mice (0.28 ± 0.01 μm^2; P<0.0001 vs AAV9-Con). Similar findings were obtained for the T-tubule power, which is a measure of the integrity of the T-tubule structure in myocytes [14]. The normalized T-tubule power was reduced in AAV9-Con treated TAC mice (0.83 ± 0.04) compared to sham mice (1.00 ± 0.05; P=0.02; Fig. 5D). In contrast, treatment with AAV9-JPH2 caused

normalization of the T-tubule power (0.97 ± 0.04; P=0.04). Thus, treatment with AAV9 to restore JPH2 levels in failing hearts rescues the deficiencies in the T-tubule network.

3.6. AAV9-JPH2 improves SR Ca^{2+} handling in cardiomyocytes from TAC mice

We next assessed the potential impact of AAV9-JPH2 gene therapy on SR Ca^{2+} handling in ventricular myocytes. When isolated cardiomyocytes were paced at 1 Hz, the Ca^{2+} transient amplitude was significantly lower in AAV9-Con treated TAC mice (1.51 ± 0.06) compared to sham mice (1.70 ± 0.04; P<0.05; Fig. 6A–B). Treatment with AAV9-JPH2 normalized the Ca^{2+} transient amplitude (1.74 ± 0.08; P=0.02 vs AAV9-Con). The SR Ca^{2+} load as measured by the caffeine dump protocol was also significantly lower in AAV9-Con treated TAC mice (2.03 ±0.13) compared to sham mice (3.19 ± 0.23; P<0.0001; Fig. 6C). A partial, non-significant improvement of the SR Ca^{2+} load was observed in myocytes from AAV9-JPH2 treated TAC mice (2.44 ± 0.15; P=0.23 vs. AAV9-Con). Finally, we measured the activity of the Na^{+}/Ca^{2+}-exchanger (NCX) by calculating the inverse of the decay time constant of the caffeine-induced SR Ca^{2+} transient [18]. Compared to sham mice (1.00 ± 0.13), there was a trend towards enhanced NCX activity in the AAV9-Con treated TAC mice (1.62 ± 0.26; P=0.26; Fig. 6D). Treatment of TAC mice with AAV9-JPH2, on the other hand, normalized NCX activity to levels (1.11 ± 0.27) similar to those seen in sham mice. Taken together, overexpression of JPH2 in the hearts of mice subjected to TAC for the most part restored SR Ca^{2+} handling dynamics.

3.7. AAV9-JPH2 gene therapy suppresses abnormal SR Ca^{2+} release in cardiomyocytes from TAC mice

In order to determine whether attenuated spontaneous Ca^{2+} leak from RyR2 was responsible for improved systolic Ca^{2+} handling in AAV9-JPH2 treated mice, we assessed the frequency of elementary Ca^{2+} release events (Ca^{2+} sparks) in myocytes isolated from the different groups of mice. The Ca^{2+} spark frequency (CaSpF) was significantly increased in AAV9-Con treated TAC mice (2.02 ± 0.26) compared to sham controls (3.68 ± 0.63; P<0.05; Fig. 7A–B). In contrast, treatment with AAV9-JPH2 normalized the CaSpF (2.11 ± 0.22; P<0.05 vs AAV9-Con) to levels similar to sham mice. The amplitude of the Ca^{2+} sparks was also significantly increased in AAV9-Con treated TAC mice (0.338 ± 0.006) compared to sham mice (0.273 ± 0.004; P<0.001; Fig. 7C). The spark amplitude was partially rescued by AAV9-JPH2 treatment (0.316 ± 0.007; P<0.05 vs. AAV9-Con), although the amplitude was still greater than those in sham mice. Further analysis revealed that the Ca^{2+} spark full width half maximum (FWHM) was increased in AAV9-Con treated TAC mice (1.85 ± 0.06) compared to sham mice (1.64 ± 0.06; P<0.05; Fig. 7D), whereas AAV9-JPH2 treatment did not exhibited increased FWHM (1.74 ± 0.06; P=0.60 vs. sham).

3.8. AAV9-JPH2 increases JPH2 levels in TAC mice and ameliorates downstream hypertrophic responses

We performed western blotting to assess JPH2 proteins levels in the different groups of mice. As expected, reduced JPH2 expression (normalized to housekeeping gene GADPH) was found in AAV9-Con treated TAC mice (0.72 ± 0.08) compared to sham controls (1.00 ± 0.03; P<0.05; Fig. 8A–B). In contrast, AAV9-JPH2 gene therapy increased cardiac JPH2 levels (1.14 ± 0.06), which was significantly higher than AAV9-Con mice (P<0.01). Thus,

cardiac gene therapy using AAV9-JPH2 causes sustained normalization of JPH2 levels up to 9-weeks after TAC (i.e., 6 weeks after AAV9 administration).

Finally, we assessed the impact of JPH2 gene therapy on hypertrophic signaling pathways. Quantitative polymerase chain reaction (qPCR) revealed increased mRNA levels of several pro-hypertrophic markers in AAV9-Con treated TAC mice compared to sham, including 'regulator of calcineurin 1 isoform 4′ (*Rcan1.4*) - a marker of 'nuclear factor of activated T cells' (NFAT) activity, myosin heavy chain 7 (*Myh7*), natriuretic peptide type A (*Nppa*), and natriuretic peptide type B (*Nppb*) (Fig. 8C–F). Treatment with AAV9-JPH2 did not appear to have an impact on *Rcan1* expression. However, AAV9-JPH2 treated hearts had significantly lower *Myh7* mRNA levels than AAV9-Con treated mice ($P<0.05$; Fig. 8D). Moreover, the downstream signaling responses were also partially ameliorated in AAV9-JPH2 treated mice with a non-significant decrease in mRNA levels of *Nppa* and *Nppb* compared to AAV9-Con treated mice.

4. DISCUSSION

This study demonstrates the potential therapeutic effects of JPH2 overexpression against adverse cardiac remodeling in a preclinical animal model of HF. Previous studies have shown the beneficial effects of transgenic JPH2 overexpression in mice subjected to experimental HF [10]. However, our current study provides a more translational perspective since JPH2 expression was increased after the onset of HF, using a gene therapy approach. Specifically, this study demonstrates that after pressure-overload induced HF, re-expression of JPH2 in cardiomyocytes is associated with maintained T-tubule organization, normalized SR Ca^{2+} handling, and a complete arrest of a further decline of cardiac dysfunction. These findings suggest that enhancing JPH2 expression using a gene-therapy approach in early HF might prevent disease progression.

4.1. Physiological role of JPH2 in JMC microdomains

Proper organization of different classes of Ca^{2+}channels within the JMC microdomain within cardiac myocytes is critical to normal cardiac function [2]. JPH2 has emerged to be a key structural protein that anchors T-tubule invaginations to junctional SR organelles, in order for efficient ECC to occur [5, 19, 20]. Moreover, JPH2 was found to be essential for T-tubulogenesis during postnatal development of the heart [3]. The expression and localization of JPH2 coincides with the maturation of cardiac Ca handling including JMC formation and generation of CICR [3, 21]. While increased levels of perinatal JPH2 were able to accelerate this maturation process, adult cardiomyocytes overexpressing JPH2 did not exhibit an altered T-tubule architecture [3]. Given the complex process of generating T-tubules, enhancement of a number of factors would likely be needed to alter the mature architecture. Within mature JMCs, JPH2 anchors T-tubule membranes via lipophilic MORN domains, and junctional SR via a C-terminal transmembrane domain [19, 22]. With increased levels of JPH2 within the JMC space, the integrity of this membrane tethering is likely enhanced due to an increase in the number of JPH2 anchoring foci.

Beyond this structural tethering role, JPH2 has a direct stabilizing interaction with RyR2 within JMCs [4, 5]. Super-resolution microscopy has shown JPH2 and RyR2 are highly co-

localized within similarly distributed, well-defined clusters. The dispersion of JPH2 within the JMC and among RyR2 clusters suggests JPH2 may be critical for proper localization of ion channels. Furthermore, a decreased ratio of JPH2:RyR2 has been implicated in the pathogenesis of atrial fibrillation [4, 5]. This suggests overexpression of JPH2 and increased JPH2 to RyR2 ratio may stabilize RyR2 and alter RyR2 clustering. Mice with overexpression of JPH2 showed a decrease in frequency and size of Ca^{2+} sparks, which can be consistent with increased RyR2 stabilization. The exact stoichiometry of the interaction between JPH2 and RyR2 is unknown at this time. Since RyR2 is a homo-tetrameric channel, it is plausible that multiple JPH2 binding sites exist with a higher percentage of these binding sites occupied in JPH2 overexpression leading to RyR2 stabilization and reduced diastolic Ca^{2+} leak [23]. Further studies using super-resolution or electron microscopy in cardiomyocytes with increased JPH2 levels would be needed to examine the morphology and localization of RyR2 within JMCs.

4.2. Role of JPH2 in adverse cardiac remodeling in heart failure

Disruption of the highly ordered cardiomyocyte ultrastructure occurs in a variety of cardiac diseases [6, 24, 25]. Studies have shown a high level of correlation between this pathological remodeling and a decrease in JPH2 expression [9, 14]. Mutations in JPH2 have been linked to both hypertrophic cardiomyopathy, in which the left ventricle thickens [26], and more recently, to dilated cardiomyopathy, a disorder in which the left ventricle dilates [27]. Moreover, downregulation of JPH2 levels has been observed in patients with hypertrophic cardiomyopathy [8]. Studies in a rodent model of HF revealed that this downregulation has been shown to be an early event suggesting decreases in JPH2 may precipitate remodeling instead of being a consequence of remodeling [28].

In failing hearts, functional uncoupling of RyR2 and LTCC prevents efficient CICR and can diminish contractile force generation, which is thought to be a primary mechanism of HF with reduced ejection fraction [29]. The nanoscale organization of ion channels is critical for normal CICR, and uncoupled “orphaned” RyRs have been linked to dyssynchronous Ca release [30]. Together it is possible that pathological stress causes the downregulation of JPH2 and the loss of structural integrity of JMCs leading to orphaned RyR2s and blunted CICR. These RyR2s both lack the stabilizing interaction of JPH2 and undergo chronic hyperphosphorylation leading to increased diastolic Ca^{2+} leak and cardiac dysfunction. Here, we showed that AAV9-JPH2 is able to ameliorate the loss of ordered T-tubules and decrease diastolic Ca^{2+} leak in a rodent pressure-overload HF model. Functionally, mice that received JPH2 gene therapy had a preserved ejection fraction compared to mice that received AAV9-Con. These results suggest that preservation or enhancement of JPH2-mediated membrane tethering in JMCs can prevent adverse cardiac remodeling. Preventing the orphaning of RyR2 away from associated LTCC preserves ECC, and maintaining JPH2-mediated RyR2 stabilization ameliorates pathological diastolic Ca^{2+}leak.

4.3. Possible mechanisms of JPH2 downregulation in HF

The molecular mechanisms by which JPH2 expression levels are reduced in HF are still poorly understood. It has been reported that microRNA24 (mIR-24), an immediate upstream suppressor of JPH2, is upregulated in a rat model of TAC [31]. Adenoviral overexpression of

miR-24 in rat ventricular myocytes led to downregulation of JPH2, confirming a causal relationship between high miR-24 levels and reduced JPH2 expression [31]. Moreover, *in vivo* silencing of miR-24 using a specific antagomir in mice subjected to TAC prevented the degradation of cardiac contractility, but not ventricular hypertrophy.[32] Among Ca^{2+} handling proteins, miR-24 was shown to only target the JPH2 gene, suggesting that JPH2 is required for ECC [31].

A recent study demonstrated that miR-24 is part of the intergenic miR-23a-miR-27a-miR-24-2 cluster, which is activated by the calcineurin-NFAT pathway in hypertrophic cardiomyopathy [33]. Our present study revealed that enhancing JPH2 expression – in this case by direct AAV9-mediated overexpression instead of suppressing mIR-24 – also did not revert hypertrophy of the left ventricular wall, despite beneficial effects of cardiac contractility (see Fig. 4D). Consistent with this finding, we observed elevated levels of Rcan1.4 expression, a marker of the Ca^{2+}-dependent pro-hypertrophic NFAT pathways [34]. Whereas cardiac hypertrophy was not normalized by JPH2 overexpression in TAC mice, cardiac contractility did improve following AAV9-JPH2 treatment due to normalization of T-tubule structures and intracellular Ca^{2+} cycling.

4.4. Targeted therapies for the reversal of pathological cardiac remodeling

Current therapies for HF are mostly targeted at symptomatic relief and slowing the progression of disease [35]. The typical core drug regimen for systolic HF includes an angiotensin-converting enzyme (ACE) inhibitor, beta blocker, and diuretic with the addition of ionotropic agents for management of decompensated severe HF [36]. A few of these therapies (predominantly ACE-inhibitors and beta blockers) have been shown to mildly induce reverse remodeling and improve cardiac function [37]. In certain modifiable etiologies of HF, removal of the pathological stress can result in recovery of cardiac function. Interestingly, cardiac resynchronization therapy was able to reverse T-tubule remodeling in a canine HF model [38]. However, the precise mechanisms for such improvements are unknown.

Aside from pharmacological treatment of HF, gene therapy has been an attractive option for a targeted therapeutic approach to ameliorating HF. SERCA2a has been investigated as a potential candidate for gene therapy due to its involvement in ECC. During a recent phase 2b clinical trial, however, SERCA2a gene therapy failed to improve markers of cardiac function over the placebo in patients with advanced HF. Despite the importance of SERCA2a in maintaining the input of SR Ca^{2+} stores, there are several issues, which may have prevented the desired outcomes for this trial. For example, it is possible that increasing SERCA2a did not normalize JPH2 levels and the loss of T-tubule architecture, which may be a requirement for reverse remodeling. However, carefully controlled experiments in large animal models of HF will be needed to test this hypothesis. Nevertheless, our study demonstrated that JPH2 gene therapy can improve outcomes in mice in when treated in the early stages of HF. The AAV9 serotype has a high native tropism for cardiac cells [39]. Our studies demonstrated an increase in cardiac JPH2 expression 2 weeks after tail vein injection and therapeutic potential in a mouse with mild cardiac remodeling.

4.6. Conclusions

Our findings suggest that AAV9-JPH2 mediated gene therapy constitutes a therapeutic strategy against adverse cardiac remodeling in a preclinical model of heart failure. Enhanced expression of JPH2 ameliorated the loss of T-tubule architecture and improved SR Ca^{2+} leak associated with contractile failure in mice following TAC. Moreover, AAV9-JPH2 enhanced Ca^{2+} transients and ultimately cardiac function in TAC mice. This may be mediated by an increased integrity of tethering between T-tubule and SR membranes, and a preserved or increased stabilization of RyR2 within JMCs. These findings suggest that targeting JPH2-mediated JMC integrity might be an attractive therapeutic approach for pathological cardiac remodeling.

Acknowledgments

This project was supported by the Mouse Phenotyping Core at Baylor College of Medicine with funding from the NIH (U54 HG006348).

7. FUNDING SOURCES

This work was supported by an Established Investigator Award (13EIA14560061) of the American Heart Association (to X.H.T.W), grants from the NIH/NHLBI (R01-HL089598, R01-HL091947, R01-HL117641, and R41-HL129570 to X.H.T.W.; R01-HL75573, R01-HL104535, and P01-HL085577 to C.C.G.), and A.Q. was supported by AHA predoctoral fellowship 14PRE20490083. D.B. was supported by AHA predoctoral fellowship 12PRE12030237. A.Q. and D.B. were supported by NIH grant T32HL007676-21. SD was supported an Excellence Grant from the German Centre for Cardiovascular Research (DZHK).

References

1. Ather S, Respress JL, Li N, Wehrens XH. Alterations in ryanodine receptors and related proteins in heart failure. Biochim Biophys Acta. 2013; 1832:2425–31. [PubMed: 23770282]
2. Scriven DR, Asghari P, Moore ED. Microarchitecture of the dyad. Cardiovasc Res. 2013; 98:169–76. [PubMed: 23400762]
3. Reynolds JO, Chiang DY, Wang W, Beavers DL, Dixit SS, Skapura DG, et al. Junctophilin-2 is necessary for T-tubule maturation during mouse heart development. Cardiovasc Res. 2013; 100:44–53. [PubMed: 23715556]
4. Beavers DL, Wang W, Ather S, Voigt N, Garbino A, Dixit SS, et al. Mutation E169K in junctophilin-2 causes atrial fibrillation due to impaired RyR2 stabilization. J Am Coll Cardiol. 2013; 62:2010–9. [PubMed: 23973696]
5. van Oort RJ, Garbino A, Wang W, Dixit SS, Landstrom AP, Gaur N, et al. Disrupted junctional membrane complexes and hyperactive ryanodine receptors after acute junctophilin knockdown in mice. Circulation. 2011; 123:979–88. [PubMed: 21339484]
6. He J, Conklin MW, Foell JD, Wolff MR, Haworth RA, Coronado R, et al. Reduction in density of transverse tubules and L-type Ca(2+) channels in canine tachycardia-induced heart failure. Cardiovasc Res. 2001; 49:298–307. [PubMed: 11164840]
7. Wu HD, Xu M, Li RC, Guo L, Lai YS, Xu SM, et al. Ultrastructural remodelling of Ca(2+) signalling apparatus in failing heart cells. Cardiovasc Res. 2012; 95:430–8. [PubMed: 22707157]
8. Landstrom AP, Kellen CA, Dixit SS, van Oort RJ, Garbino A, Weisleder N, et al. Junctophilin-2 expression silencing causes cardiocyte hypertrophy and abnormal intracellular calcium-handling. Circ Heart Fail. 2011; 4:214–23. [PubMed: 21216834]
9. Minamisawa S, Oshikawa J, Takeshima H, Hoshijima M, Wang Y, Chien KR, et al. Junctophilin type 2 is associated with caveolin-3 and is down-regulated in the hypertrophic and dilated cardiomyopathies. Biochem Biophys Res Comm. 2004; 325:852–6. [PubMed: 15541368]

10. Guo A, Zhang X, Iyer VR, Chen B, Zhang C, Kutschke WJ, et al. Overexpression of junctophilin-2 does not enhance baseline function but attenuates heart failure development after cardiac stress. Proc Natl Acad Sci U S A. 2014; 111:12240–5. [PubMed: 25092313]
11. Respress JL, Wehrens XH. Transthoracic echocardiography in mice. J Vis Exp. 2010:1738. [PubMed: 20517201]
12. Doroudgar S, Volkers M, Thuerauf DJ, Khan M, Mohsin S, Respress JL, et al. Hrd1 and ER-Associated Protein Degradation, ERAD, Are Critical Elements of the Adaptive ER Stress Response in Cardiac Myocytes. Circ Res. 2015 In press.
13. Picht E, Zima AV, Blatter LA, Bers DM. SparkMaster: automated calcium spark analysis with ImageJ. Am J Physiol Cell Physiol. 2007; 293:C1073–81. [PubMed: 17376815]
14. Wei S, Guo A, Chen B, Kutschke W, Xie YP, Zimmerman K, et al. T-tubule remodeling during transition from hypertrophy to heart failure. Circ Res. 2010; 107:520–31. [PubMed: 20576937]
15. Muller OJ, Leuchs B, Pleger ST, Grimm D, Franz WM, Katus HA, et al. Improved cardiac gene transfer by transcriptional and transductional targeting of adeno-associated viral vectors. Cardiovasc Res. 2006; 70:70–8. [PubMed: 16448634]
16. van Oort RJ, Respress JL, Li N, Reynolds C, De Almeida AC, Skapura DG, et al. Accelerated development of pressure overload-induced cardiac hypertrophy and dysfunction in an RyR2-R176Q knockin mouse model. Hypertension. 2010; 55:932–8. [PubMed: 20157052]
17. Respress JL, van Oort RJ, Li N, Rolim N, Dixit SS, deAlmeida A, et al. Role of RyR2 phosphorylation at S2814 during heart failure progression. Circ Res. 2012; 110:1474–83. [PubMed: 22511749]
18. Voigt N, Li N, Wang Q, Wang W, Trafford AW, Abu-Taha I, et al. Enhanced sarcoplasmic reticulum Ca2+ leak and increased Na+-Ca2+ exchanger function underlie delayed afterdepolarizations in patients with chronic atrial fibrillation. Circulation. 2012; 125:2059–70. [PubMed: 22456474]
19. Takeshima H, Komazaki S, Nishi M, Iino M, Kangawa K. Junctophilins: a novel family of junctional membrane complex proteins. Mol Cell. 2000; 6:11–22. [PubMed: 10949023]
20. Garbino A, Wehrens XH. Emerging role of junctophilin-2 as a regulator of calcium handling in the heart. Acta Pharmacol Sin. 2010; 31:1019–21. [PubMed: 20694023]
21. Ziman AP, Gomez-Viquez NL, Bloch RJ, Lederer WJ. Excitation-contraction coupling changes during postnatal cardiac development. J Mol Cell Cardiol. 2010; 48:379–86. [PubMed: 19818794]
22. Garbino A, van Oort RJ, Dixit SS, Landstrom AP, Ackerman MJ, Wehrens XH. Molecular evolution of the junctophilin gene family. Physiol Genomics. 2009; 37:175–86. [PubMed: 19318539]
23. Van Petegem F. Ryanodine receptors: structure and function. J Biol Chem. 2012; 287:31624–32. [PubMed: 22822064]
24. Lyon AR, MacLeod KT, Zhang Y, Garcia E, Kanda GK, Lab MJ, et al. Loss of T-tubules and other changes to surface topography in ventricular myocytes from failing human and rat heart. Proc Natl Acad Sci U S A. 2009; 106:6854–9. [PubMed: 19342485]
25. Zhang HB, Li RC, Xu M, Xu SM, Lai YS, Wu HD, et al. Ultrastructural uncoupling between T-tubules and sarcoplasmic reticulum in human heart failure. Cardiovasc Res. 2013; 98:269–76. [PubMed: 23405000]
26. Landstrom AP, Weisleder N, Batalden KB, Bos JM, Tester DJ, Ommen SR, et al. Mutations in JPH2-encoded junctophilin-2 associated with hypertrophic cardiomyopathy in humans. J Mol Cell Cardiol. 2007; 42:1026–35. [PubMed: 17509612]
27. Sabater-Molina M, Navarro M, Garcia-Molina Saez E, Garrido I, Pascual-Figal D, Gonzalez Carrillo J, et al. Mutation in JPH2 cause dilated cardiomyopathy. Clin Genet. 2016
28. Xu M, Zhou P, Xu SM, Liu Y, Feng X, Bai SH, et al. Intermolecular failure of L-type Ca2+ channel and ryanodine receptor signaling in hypertrophy. PLoS Biol. 2007; 5:e21. [PubMed: 17214508]
29. Gomez AM, Valdivia HH, Cheng H, Lederer MR, Santana LF, Cannell MB, et al. Defective excitation-contraction coupling in experimental cardiac hypertrophy and heart failure. Science. 1997; 276:800–6. [PubMed: 9115206]

30. Song LS, Sobie EA, McCulle S, Lederer WJ, Balke CW, Cheng H. Orphaned ryanodine receptors in the failing heart. Proc Natl Acad Sci U S A. 2006; 103:4305–10. [PubMed: 16537526]
31. Xu M, Wu HD, Li RC, Zhang HB, Wang M, Tao J, et al. Mir-24 regulates junctophilin-2 expression in cardiomyocytes. Circ Res. 2012; 111:837–41. [PubMed: 22891046]
32. Li RC, Tao J, Guo YB, Wu HD, Liu RF, Bai Y, et al. In vivo suppression of microRNA-24 prevents the transition toward decompensated hypertrophy in aortic-constricted mice. Circ Res. 2013; 112:601–5. [PubMed: 23307820]
33. Hernandez-Torres F, Aranega AE, Franco D. Identification of regulatory elements directing miR-23a-miR-27a-miR-24-2 transcriptional regulation in response to muscle hypertrophic stimuli. Biochim Biophys Acta. 2014; 1839:885–97. [PubMed: 25050919]
34. Li N, Chiang DY, Wang S, Wang Q, Sun L, Voigt N, et al. Ryanodine-Receptor Mediated Calcium Leak Drives Progressive Development of an Atrial Fibrillation Substrate in a Transgenic Mouse Model. Circulation. 2014
35. McMurray JJ. Clinical practice. Systolic heart failure. N Engl J Med. 2010; 362:228–38. [PubMed: 20089973]
36. Jessup M, Abraham WT, Casey DE, Feldman AM, Francis GS, Ganiats TG, et al. 2009 focused update: ACCF/AHA Guidelines for the Diagnosis and Management of Heart Failure in Adults: a report of the American College of Cardiology Foundation/American Heart Association Task Force on Practice Guidelines: developed in collaboration with the International Society for Heart and Lung Transplantation. Circulation. 2009; 119:1977–2016. [PubMed: 19324967]
37. Remme WJ, Riegger G, Hildebrandt P, Komajda M, Jaarsma W, Bobbio M, et al. The benefits of early combination treatment of carvedilol and an ACE-inhibitor in mild heart failure and left ventricular systolic dysfunction. The carvedilol and ACE-inhibitor remodelling mild heart failure evaluation trial (CARMEN). Cardiovasc Drugs Ther. 2004; 18:57–66. [PubMed: 15115904]
38. Sachse FB, Torres NS, Savio-Galimberti E, Aiba T, Kass DA, Tomaselli GF, et al. Subcellular structures and function of myocytes impaired during heart failure are restored by cardiac resynchronization therapy. Circ Res. 2012; 110:588–97. [PubMed: 22253411]
39. Bish LT, Morine K, Sleeper MM, Sanmiguel J, Wu D, Gao G, et al. Adeno-associated virus (AAV) serotype 9 provides global cardiac gene transfer superior to AAV1, AAV6, AAV7, and AAV8 in the mouse and rat. Hum Gene Ther. 2008; 19:1359–68. [PubMed: 18795839]

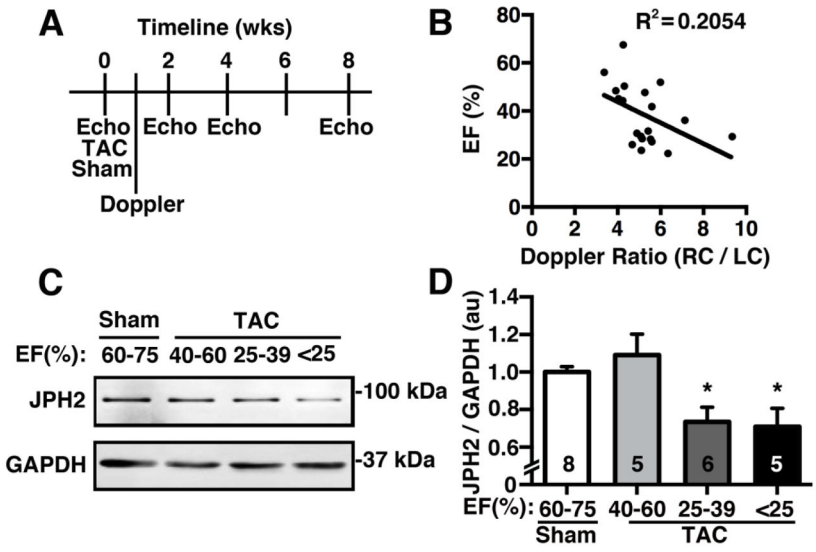

Figure 1.

Pressure-overload induced heart failure leads to decline in JPH2 expression. (A) Summary of study design for transverse aortic constriction (TAC) study in mice. (B) Correlation of Doppler ratios (right carotid/left carotid flow ratio) with ejection fraction (EF) at 8 weeks post TAC. (C) Representative Western blot and (D) quantification of JPH2 protein levels in ventricles of mice subjected to sham procedure (EF:60–75%), or TAC resulting in mild (EF: 40–60%), moderate (EF: 25–39%), or severe (EF: <25%) heart failure. Numbers in bars = number hearts. *P<0.05 compared to sham group.

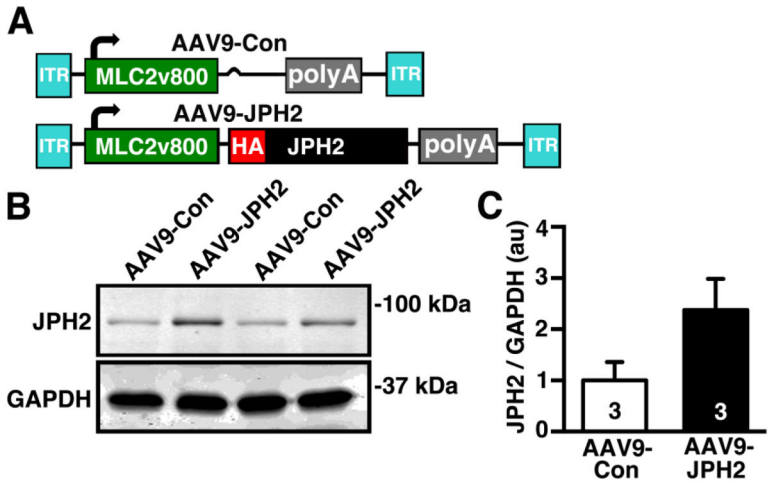

Figure 2.

AAV9 vector used to overexpress JPH2 in mouse hearts. (A) Junctophilin-2 (AAV9-JPH2) AAV9 vector featuring a cardiac-specific MLC2v800 promoter, N-terminal hemagglutinin (HA) tagged-JPH2, with polyA tail and inverted tandem repeats (ITR). The control (AAV9-Con) vector contains the same elements except for the HA-JPH2 sequence. (B) Representative Western blot showing JPH2 protein levels in ventricular lysates from WT mice transduced with 1×10^{11} genome-containing units (GCU) by tail vein injection of AAV9-Con or AAV9-JPH2. (C) Quantification of JPH2 protein levels. Number in bars= number hearts.

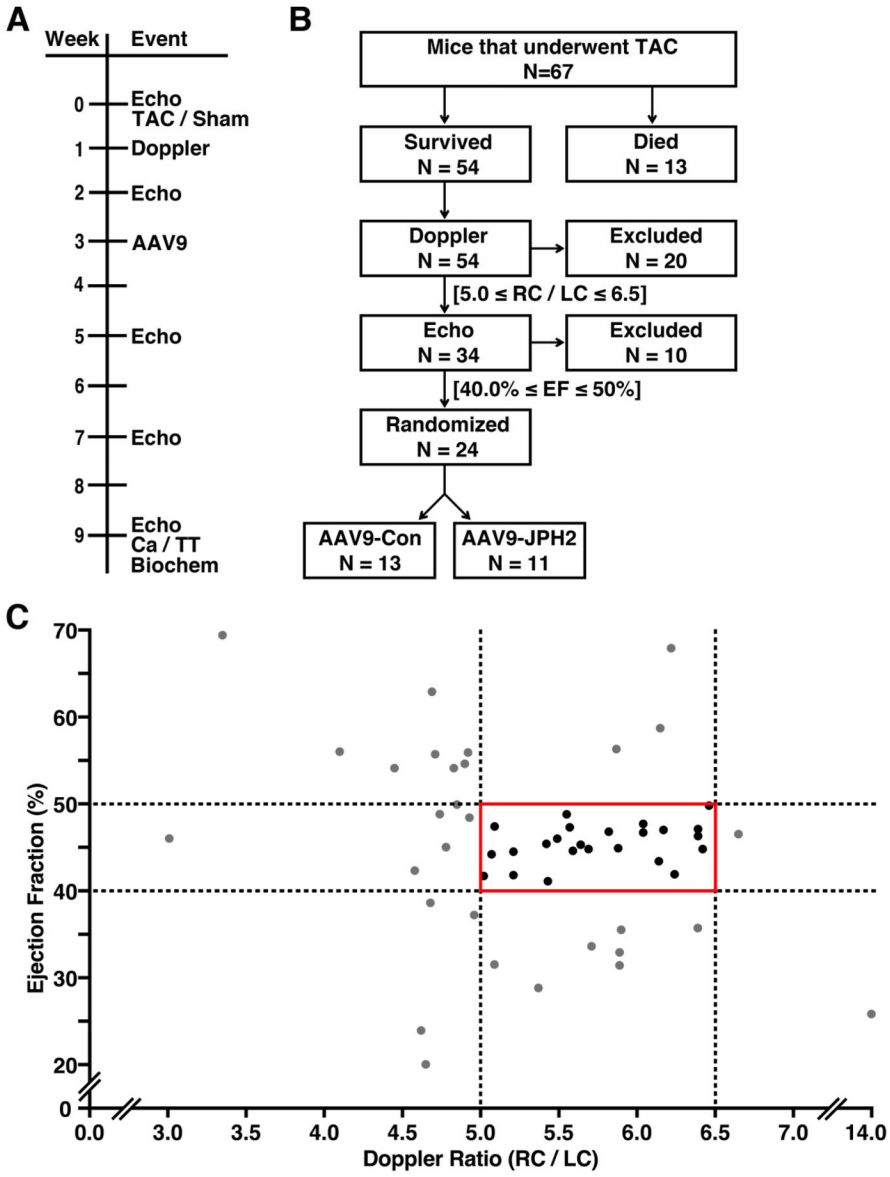

Figure 3.

Study design for gene therapy study in a mouse model of heart failure. (A) Timeline depicting various experimental procedures performed on a cohort of mice subjected to sham or transverse aortic constriction (TAC), and subsequent AAV9 gene therapy. (B) Flow chart of sequential inclusion criteria used to obtain a cohort of mice with similar levels of early stage heart failure that were then randomized to receive AAV9-Con or AAV9-JPH2. Criteria included Doppler ratio of right carotid to left carotid peak velocity (RC/LC) and echocardiographic ejection fraction (EF). (C) Graph showing distribution of individual mouse Doppler ratios at 1-week post-TAC and EF assessed by echo at 2-weeks post TAC. The solid red box denotes the group of mice that were included for randomization. Black dots represent mice included and grey dots denote mice excluded from the trial based on Doppler and echo criteria. N= number mice.

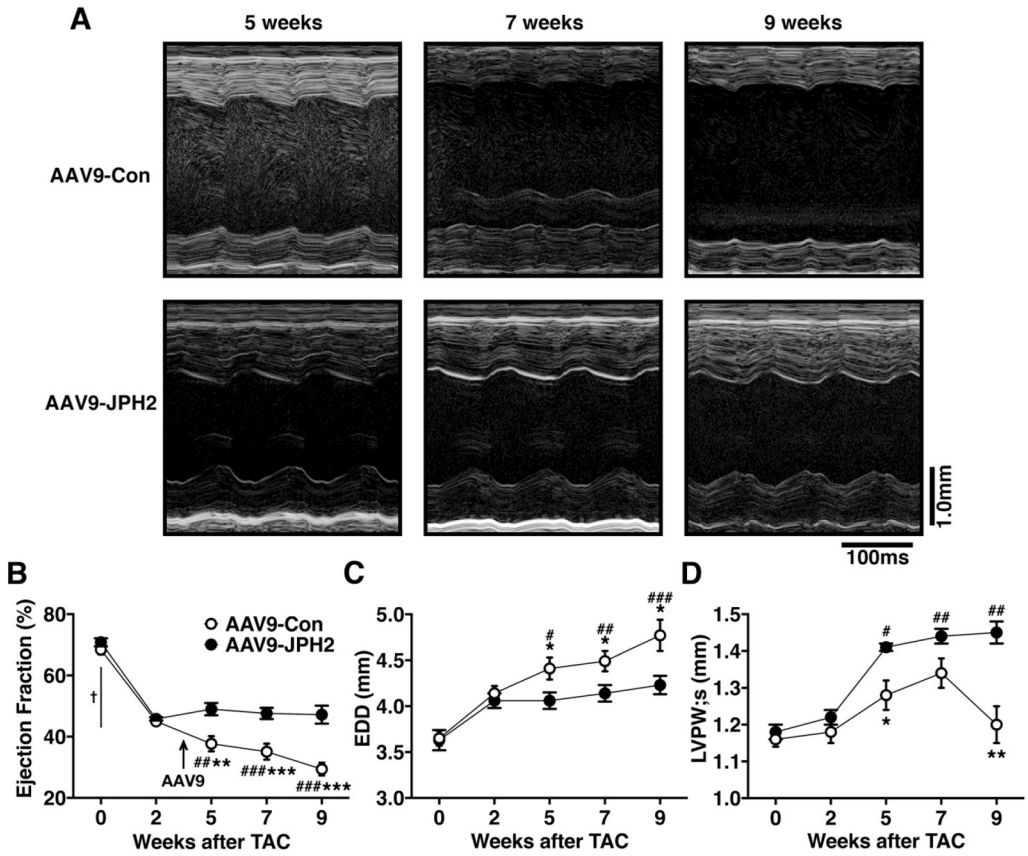

Figure 4.

AAV9-JPH2 gene therapy maintains cardiac function after pressure-overload induced pathological remodeling. (A) Representative M-mode echocardiograms of AAV9-Con or AAV9-JPH2 treated mice at 5, 7, and 9 weeks post-TAC. Quantification of (B) ejection fraction (EF), (C) end-diastolic diameter (EDD), and (D) systolic left ventricular posterior wall thickness (LVPW;s) at baseline (0) and 2, 5, 7, and 9 weeks post-TAC. Arrow indicates time of AAV9-JPH2 injection at 3 weeks post-TAC. N=number mice. *P<0.05, **P<0.01, ***P<0.001 between treatment groups at a single time-point; † P<0.0001 for all groups compared to baseline; # P<0.05 and ## P<0.01, ### P<0.001 within groups compared to 2 weeks post-TAC.

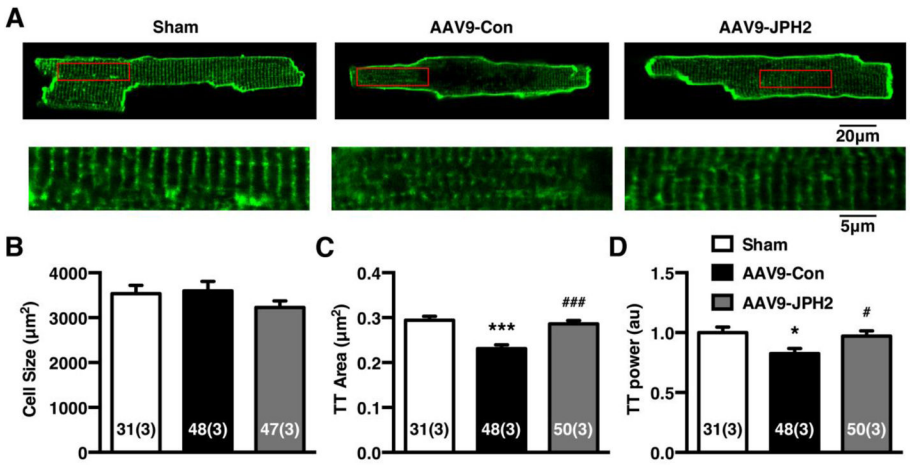

Figure 5.

AAV9-JPH2 therapy attenuates transverse-tubule (T-tubule) remodeling in TAC mice. (A) Representative T-tubule images of isolated ventricular cardiomyocytes stained with di-8-ANEPPS from mice 9 weeks post sham or TAC, treated with AAV9-Con or AAV9-JPH2. Insets are magnifications of corresponding boxed regions in T-tubule images. (B) Average cell size, (C) T-tubule area (TT Area), and (D) normalized T-tubule power spectrum analysis (TT Power) of isolated cells from sham and differentially treated TAC mice. Numbers in each bar = number of cells (number of mice). *P<0.05, ***P<0.001 sham vs TAC; # P<0.05, ### P< 0.001 AAV9-Con vs AAV9-JPH2.

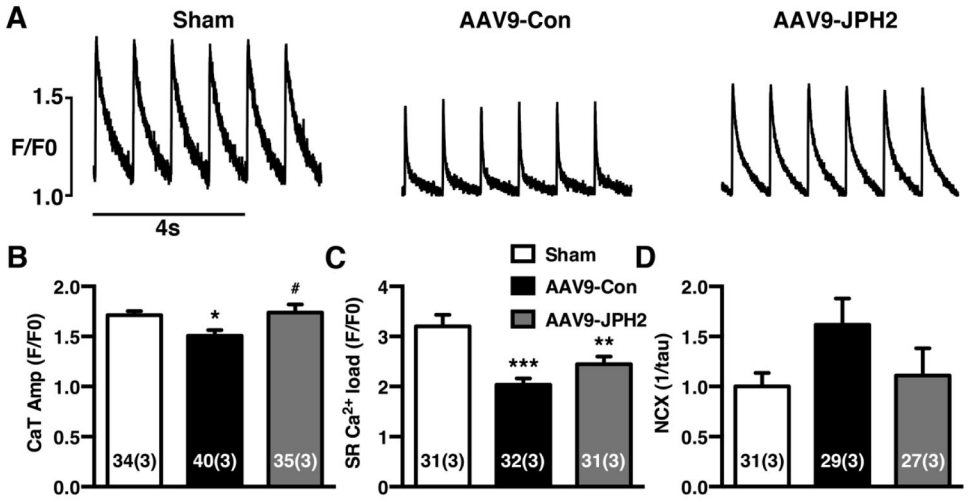

Figure 6.

AAV9-JPH2 improves SR Ca^{2+} handling in cardiomyocytes from TAC mice. (A) Representative cytosolic Ca^{2+} traces at 1-Hz pacing from isolated cardiomyocytes from sham or mice treated with AAV9-Con or AAV9-JPH2 following TAC. (B) Average Ca^{2+} transient amplitude, (C) SR Ca^{2+} load, and (D) Na^{+}/Ca^{2+}-exchanger (NCX) activity for each group. Numbers in each bar = number of cells (number of mice). *P<0.05, **P<0.01, ***P<0.001 sham vs TAC; #P<0.05 AAV9-Con vs AAV9-JPH2.

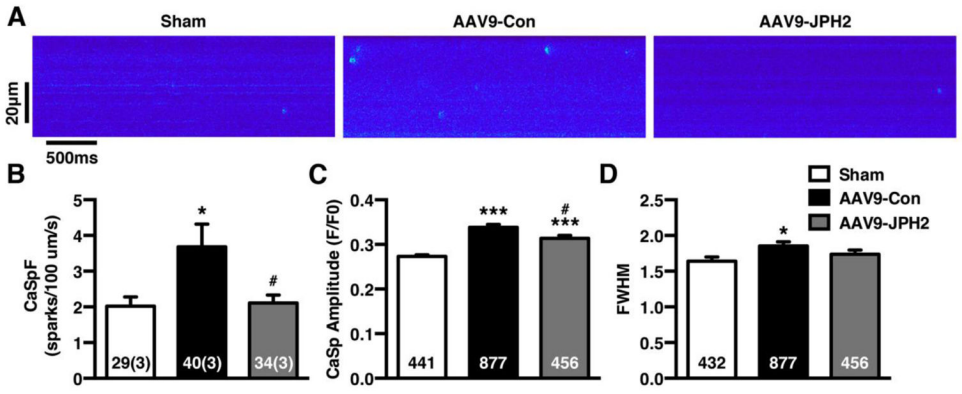

Figure 7.

AAV9-JPH2 gene therapy suppresses abnormal SR Ca^{2+} release in cardiomyocytes from TAC mice. (A) Representative confocal line scan images of Ca^{2+} sparks recorded from ventricular myocytes obtained from shams (left), and TAC mice treated with AAV9-Con (middle) and AAV9-JPH2 (right) mice. (B) Bar graph showing mean Ca^{2+} spark frequency (CaSpF), (C) Ca^{2+} spark amplitude, and (D) full-width half-maximum (FWHM) of Ca^{2+} sparks. Numbers in each bar = number of cells (number of mice) or number sparks (C–D). *P<0.05, ***P<0.001 sham vs TAC; #P<0.05 AAV9-Con vs AAV9-JPH2.

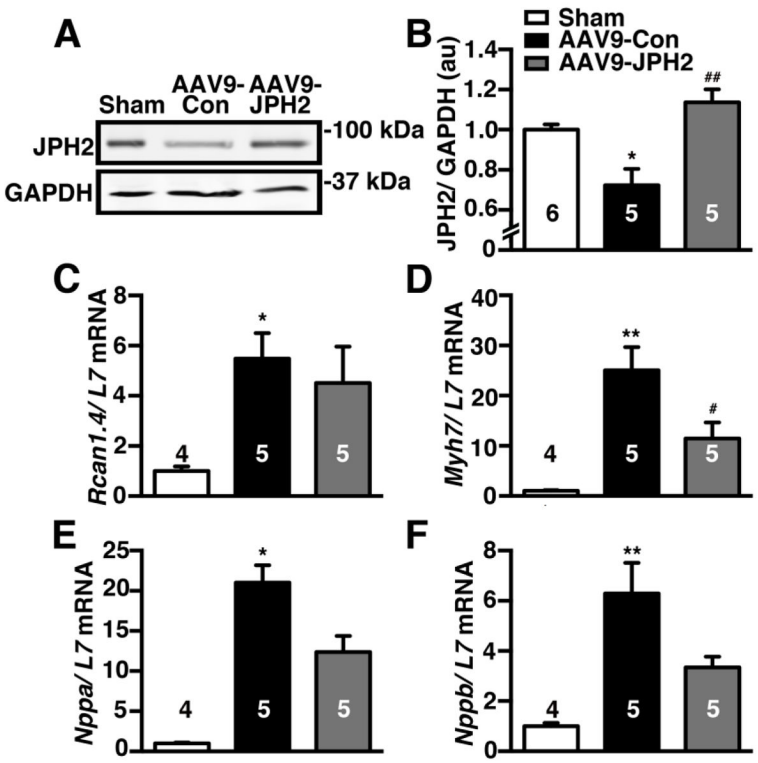

Figure 8.

AAV9-JPH2 increases JPH2 levels in TAC mice and ameliorates downstream hypertrophic responses. (A) Representative images and (B) quantification of Western blots of JPH2 protein levels in heart lysates from sham, and AAV9-Con or AAV9-JPH2 treated TAC mice. GAPDH was used as a loading control. (C) Quantitative polymerase chain reaction (qPCR) analysis of pro-hypertrophic genes including regulator of calcineurin-1 isoform 4 (*Rcan1.4*), (D) (β-myosin heavy chain (*Myh7*), (E) atrial natriuretic factor (*Nppa*), and (F) brain natriuretic peptide (*Nppb*) normalized to *L7* control Numbers in each bar = number of hearts. *P<0.05, **P<0.01 sham vs TAC; #P<0.05, ##P<0.01 AAV9-Con vs AAV9-JPH2.

Table 1

Baseline echocardiographic measurements for mice before sham or TAC procedures.

Parameter	Sham	TAC mice	P-Value
	n = 10	n = 24	
HR (bpm)	559 ± 18.54	544 ± 6.71	0.33
EF (%)	71.7 ± 1.14	69.5 ± 1.04	0.23
FS (%)	40.1 ± 0.87	38.6 ± 0.85	0.29
ESD (mm)	2.11 ± 0.08	2.25 ± 0.06	0.23
EDD (mm)	3.51 ± 0.08	3.64 ± 0.06	0.26
LVAW;d (mm)	0.78 ± 0.02	0.83 ± 0.02	0.11
LVAW;s (mm)	1.01 ± 0.02	1.05 ± 0.03	0.31
LVID;d (mm)	3.42 ± 0.08	3.54 ± 0.06	0.23
LVID;s (mm)	2.16 ± 0.08	2.27 ± 0.06	0.34
LVPW;d (mm)	0.78 ± 0.02	0.81 ± 0.02	0.30
LVPW;s (mm)	1.23 ± 0.02	1.17 ± 0.02	0.12

EDD: end-diastolic diameter; EF: ejection fraction; ESD: end-systolic diameter; FS: fractional shortening, HR: heart rate, LVAW;d/LVAW;s: left ventricular anterior wall in diastole/systole; LVID;d/LVID;s: left ventricular internal diameter in diastole/systole; LVPW;d/LVPW;s: left ventricular posterior wall in diastole/systole.

Table 2

Echocardiographic measurements for sham, AAV9-Con and AAV9-JPH2 treated TAC mice at 9 weeks post TAC.

Parameter	Sham	AAV9-Con	AAV9-JPH2	P-Value	P-Value	P-Value
	n = 10	n = 13	n = 11	Sham vs. AAV9-Con	Sham vs. AAV9-JPH2	AAV9-Con vs. AAV9-JPH2
HR (bpm)	565 ± 7.30	586 ± 9.01	581 ± 9.21	0.22	0.43	0.91
EF (%)	69.7 ± 0.83	29.4 ± 2.09	47.2 ± 2.93	< 0.0001	< 0.0001	< 0.0001
FS (%)	38.5 ± 0.63	13.8 ± 1.05	23.7 ± 1.75	< 0.0001	<0.0001	<0.0001
ESD (mm)	2.19 ± 0.05	4.13 ± 0.19	3.24 ± 0.14	< 0.0001	0.0001	0.0004
EDD (mm)	3.56 ± 0.06	4.77 ± 0.17	4.23 ± 0.10	< 0.0001	0.003	0.01
LVAW;d (mm)	0.72 ± 0.01	0.87 ± 0.04	0.97 ± 0.03	0.003	< 0.0001	0.06
LVAW;s (mm)	0.98 ± 0.02	1.03 ± 0.05	1.16 ± 0.04	0.69	0.01	0.05
LVID;d (mm)	3.53 ± 0.06	4.74 ± 0.16	4.16 ± 0.10	< 0.0001	0.01	0.01
LVID;s (mm)	2.29 ± 0.05	4.13 ± 0.18	3.27 ± 0.14	< 0.0001	0.0003	0.001
LVPW;d (mm)	0.81 ± 0.02	0.99 ± 0.04	1.13 ± 0.06	0.02	< 0.0001	0.07
LVPW;s (mm)	1.24 ± 0.02	1.2 ± 0.05	1.45 ± 0.07	0.82	0.03	0.004

EDD: end-diastolic diameter; EF: ejection fraction; ESD: end-systolic diameter; FS: fractional shortening, HR: heart rate, LVAW;d/LVAW;s: left ventricular anterior wall in diastole/systole; LVID;d/LVID;s: left ventricular internal diameter in diastole/systole; LVPW;d/LVPW;s: left ventricular posterior wall in diastole/systole.